

**Cytochrome P450 2E1 (CYP2E1) is the Principal Enzyme Responsible
for Urethane Metabolism: Comparative Studies Using CYP2E1-Null
and Wild-Type Mice**

Undi Hoffler, Hisham A El-Masri, and Burhan I Ghanayem

Department of Pharmacology (U.H., B.I.G.)

Meharry Medical College

Nashville, TN

and

Computational Toxicology Laboratory (H.A.E.)

Division of Toxicology

Agency for Toxic Substances and Disease Registry⁴

Atlanta, GA

and

Laboratory of Pharmacology and Chemistry (U.H., B.I.G.)

National Institute of Environmental Health Sciences

National Institutes of Health

RTP, NC

Running Title: P450 2E1 is the Principal Urethane Metabolizing Enzyme

To Whom Correspondence should be addressed

Dr. Burhan I. Ghanayem

Environmental Toxicology Program

National Institute of Environmental Health Sciences

National Institutes of Health

Research Triangle Park, NC 27709

Phone: (919) 541-3369

Fax: (919) 541-4632

ghanayem@niehs.nih.gov

31 Pages, 5 Figures, 4 Tables

Words: *Abstract* **247**
 Introduction **735**
 Discussion **1500**

Abbreviations: P450, cytochrome P450; CYP2E1-null, cytochrome P450 2E1-null mice; ABT, 1-aminobenzotriazole.

Section: *Absorption, Distribution, Metabolism, & Excretion*

Abstract

Urethane is a fermentation by-product in alcoholic beverages and foods and is classified as reasonably anticipated to be a human carcinogen. Early studies indicated that while CYP2E1 is involved, esterases are the primary enzymes responsible for urethane metabolism. Using CYP2E1-null mice, current studies were undertaken to elucidate CYP2E1's contribution to urethane metabolism. Carbonyl-¹⁴C-urethane was administered by gavage to male CYP2E1-null and wild-type mice at 10 or 100 mg/kg and its metabolism and disposition were investigated. CO₂ was confirmed as the main metabolite of urethane. Significant inhibition of urethane metabolism to CO₂ occurred in CYP2E1-null vs. wild-type mice. Pharmacokinetic modeling of ¹⁴CO₂ exhalation data revealed that CYP2E1 is responsible for approximately 96% of urethane metabolism to CO₂ in wild-type mice. The contributions of other enzymes to urethane metabolism merely account for the remaining 4%. The half-life of urethane in wild-type and CYP2E1-null mice was estimated at 0.8 and 22 hr, respectively. Additionally, the concentration of urethane-derived radioactivity in blood and tissues was dose-dependent and significantly higher in CYP2E1-null mice. HPLC analysis showed only urethane in the plasma and liver extracts of CYP2E1-null mice. Because the lack of CYP2E1 did not completely inhibit urethane metabolism, the disposition of 10 mg/kg urethane was compared in mice pretreated with the P450 inhibitor, 1-aminobenzotriazole or the esterase inhibitor, paraoxon. Unlike paraoxon, 1-Aminobenzotriazole resulted in significant inhibition of urethane metabolism to CO₂ in both genotypes. In conclusion, this work demonstrated that CYP2E1 and not esterase is the principal enzyme responsible for urethane metabolism.

Urethane (ethyl carbamate) has been used in humans as a hypnotic agent and for the treatment of varicose veins, chronic leukemia and multiple myeloma (IARC 1974). Commercially, urethane has been utilized as a co-solvent for pesticides, fumigants, and cosmetics as well as an agent to impart wash and wear properties to fabrics (Benson and Beland 1997). Urethane is also formed as a by-product of fermentation processes and is found in tobacco leaves and smoke. Currently the greatest risk of human exposure to urethane is through consumption of alcoholic beverages and fermented foods (Benson and Beland 1997). Under normal dietary conditions, free of alcoholic beverages, urethane intake in adults was approximately 20 ng/kg b.wt. with bread serving as the main source (Zimmerli *et al* 1986). In table wines, urethane concentrations exceeded 10 ng/g and in fruit brandies, its concentration ranged between 0.2-20.2 mg/g (Schlatter and Lutz 1990). Currently, a Reference Concentration (RfC) or Reference Dose (RfD) for acceptable human exposure levels to urethane has not been established.

Urethane is a well established animal carcinogen. Nettleship *et al*, first discovered urethane's carcinogenicity in 1943. Lung tumors, principally lung adenomas could be detected in C3H female mice within 2 to 3 months after one or two intraperitoneal injections of a minimal anesthetizing dose (1 ml/100g b.wt). Additionally, it was reported that repeated dosing of urethane produces a variety of tumor types in mice, rats, hamsters, guinea-pigs, and toads (Schmahl 1977). These findings also showed induction of tumors by urethane occurred regardless of the route of exposure. Mutagenic and teratogenic responses caused by urethane exposure have also been investigated (Schmahl 1977). Nomura (1975) presented findings from a multi-generational study demonstrating that a single subcutaneous injection of urethane

(1.0 mg/g b.wt.) on gestation day 17 caused tumor formation at multiple sites in first generation (F₁) offspring. Furthermore mating amongst F₁ mice produced a second generation exhibiting the same pattern of tumor development. Because these and other findings showed urethane is a multi-site carcinogen, it was classified as "reasonably anticipated to be a human carcinogen" (NTP 2000).

It is currently thought that metabolic activation is a pre-requisite for the development of urethane-induced tumors. As shown in Figure 1, earlier studies suggested that metabolism of urethane occurs via two major pathways (Page and Carlson 1994; Forkert and Lee 1997; Lee *et al* 1998; Yamamoto 1990). The first pathway is thought to entail oxidative metabolism of urethane catalyzed by P450s leading to the formation of vinyl carbamate (VC) (Figure 1). Subsequently, VC may undergo oxidation to produce vinyl carbamate epoxide (VCE) (Figure 1). VCE is considered as the ultimate carcinogen; binding to macromolecules; DNA, RNA, and proteins to produce adducts (Guengerich and Kim 1991). The second pathway of urethane metabolism was thought to be catalyzed by esterase and leads to the formation of CO₂, ethanol, and NH₃ (Figure 1). Interestingly, the final metabolite common to both pathways is CO₂. Studies conducted in rats (F344) and mice (A/jax and B6C3F1) by Yamamoto *et al* (1988) and Nomier *et al* (1989) using [carbonyl-¹⁴C]-urethane demonstrated that greater than 90% of the administered dose was exhaled as ¹⁴CO₂ within 24 hours. It has been proposed that the most dominant pathway for urethane metabolism to CO₂ (approximately 95%) is hydrolysis via esterase (Skipper *et al.*, 1951; Kaye 1960; Mirvish 1968; Nomier *et al.*, 1989; Salmon and Zeise 1991).

Dahl *et al* (1978) proposed that P450s were responsible for urethane's bioactivation. Studies by Guengerich and Kim (1991) focused specifically on the involvement of CYP2E1. Human liver microsomes were incubated with either urethane or VC in the presence of adenosine and a NADPH-generating system. 1,N⁶-ethenoadenosine adducts developed as a result of exposure to these chemicals. In subsequent incubations which included the CYP2E1 inhibitor, diethyldithiocarbamate, or CYP2E1 antibodies, inhibition of adduct formation was observed. Moreover, 1,N⁶-ethenoadenosine and 3,N⁴-ethenocytidine adducts were also seen *in vivo* in hepatic RNA after a single injection of 0.5-0.6 mg/g b.wt. [ethyl-1,2-³H] or [ethyl-1-¹⁴C]-urethane to 12 day old and adult male mice (Ribovich *et al.*, 1982). Generally, the current hypothesis states that while esterase is the primary enzyme responsible for urethane metabolism, CYP2E1 is responsible for urethane activation (Yamamoto *et al* 1990; Forkert and Lee 1997; and Lee *et al* 1998). In an attempt to address this hypothesis and assess the metabolic basis of urethane toxicity and carcinogenicity, present work is designed to more directly characterize the enzymes responsible for urethane metabolism using CYP2E1-null vs. wild-type mice.

Materials and Methods

Chemicals: [Carbonyl-¹⁴C]ethyl carbamate (urethane), specific activity 50mCi/mmol was obtained from NEN Life Science Products (Boston, MA). Using high performance liquid chromatography (HPLC), the radiochemical purity was determined to be greater than 99%. 1-Aminobenzotriazole (ABT), and paraoxon (PAX) were purchased from Sigma Chemical Co. All chemicals were of the best commercially available purity.

Animals and Treatments: CYP2E1-null mice were obtained from a colony developed at the Laboratories of Dr. Frank Gonzalez, National Cancer Institute, Bethesda, MD (Lee *et al.*, 1996). J1 embryonic stem cells generated from 129/Sv mice were used to generate the CYP2E1 mutant null mice (Lee *et al.*, 1996). Chimeric males were crossed with C57BL/6N females once to generate heterozygous mutant mice as F₁ hybrid. Homozygous mutant mice for CYP2E1 were generated from intercross of F₁ mice, then maintained at Charles River Laboratories (Wilmington, MA) by intercrossing of homozygous mice. Wild-type littermates obtained from the F₁ intercross were also maintained by intercrossing at Charles River Laboratories to serve as age-matched, strain-matched wild-type mice. No further backcross to either 129/Sv or C57BL/6N was performed at Charles River Laboratories. Furthermore, the nulizygosity of the CYP2E1-null mice was confirmed using Western Blot analysis as previously described (Wang *et al.*, 2002). In present work, 7-8 month old male wild-type and CYP2E1-null mice ranging in weight from 28-42 g were used. Animals were housed in facilities with a 12-hr light-dark cycle and fed NIH #31 diet and water. Both food and water were available *ad libitum* throughout the experiments. All animal care and experimentation

were conducted according to NIH guidelines (US Department of Health and Human Services, 1985).

Dosing solutions were made in tap water using a combination of both radiolabeled and unlabeled urethane. All urethane dosing solutions were made fresh and administered by gavage at either 10 or 100 mg/kg delivering 100-200 μ Ci/kg in a dose volume of 10 ml/kg. ABT was administered intraperitoneally (ip) 1 hour before urethane at a dose of 50 mg/2.5 ml saline/kg. PAX was delivered at a dose of 1 mg/10 ml saline/kg (ip) 30 minutes before radiolabeled urethane was administered via gavage.

Experimental design: Groups (4-8 animals each) of CYP2E1-null and WT mice were administered urethane by gavage as follows:

1. CYP2E1-null and wild-type mice received 10 mg urethane/kg and held for 24 hr.
2. CYP2E1-null and wild-type mice received 100 mg urethane/kg and held for 24 hr.
3. CYP2E1-null and wild-type mice received ABT at 50 mg/kg ip followed by 10mg urethane/kg and held for 24 hr.
4. CYP2E1-null and wild-type mice received PAX at 1 mg/kg ip followed by 10 mg urethane/kg and held for 24 hr.
5. CYP2E1-null mice received 10 or 100 mg urethane/kg and held for 72 hr.

Immediately after urethane administration, mice were housed in individual glass metabolism cages (Wyse Glass Specialties, Inc. Freeland, MI) for 24 or 72 hr, which allowed for the separate collection of urine, feces, and exhaled radioactivity. A vacuum system was attached to the glass cages that permitted the passage of air through the cage at a flow rate of 0.6-0.8 L/min. Air exiting the cage was passed through a series of traps. The first trap was an activated charcoal trap (SKC Inc., Eighty Four, PA) intended to adsorb organic volatiles exhaled by urethane treated mice. Air was subsequently passed through a trap containing approximately 400 ml of 7:3 (v/v) mixture of ethylene glycol monomethyl ether and ethanolamine for collection of expired 14 CO₂. A third trap

containing 400 ml ethanol was used to capture exhaled organic volatiles that were not adsorbed by the charcoal. $^{14}\text{CO}_2$ traps were changed at 1, 2, 4, 6, 8, 16, 24, 36, 48, 60, 72 hours post dosing of urethane. The ethanol trap was changed at 1, 4, 24, 48, 72 hours. All intake air was passed through solid calcium sulfate and soda lime to reduce moisture and CO_2 content, thus extending the efficiency of the trapping solutions over time. Urine and feces were collected 24, 48, and 72 hours after dosing. Charcoal traps were changed at 24 and 72 hr after dosing and stored at $-80\text{ }^\circ\text{C}$ to be analyzed at a later time.

At the end of the holding period, mice were euthanized by CO_2 asphyxiation and selected tissues were collected. Tissues were stored at -60 to $-80\text{ }^\circ\text{C}$ to be analyzed at a later time. Tissue and blood samples weighing between 25 and 50 mg were sampled in triplicate and ^{14}C content was quantitated via oxidation to $^{14}\text{CO}_2$ using a Packard Tri-Carb sample oxidizer (Packard Instruments Co., Meriden, CT). Blood collected from animals by cardiac puncture. Blood was collected from the high dose mice at 24 hr was centrifuged to separate RBC's and plasma. Urethane-derived radioactivity in plasma and RBC's was also quantitated using the tissue oxidizer. Feces were air-dried, ground to a fine powder, weighed, and similarly analyzed in triplicate. Charcoal traps were cracked open, charcoal was weighed, and analyzed in triplicates using the sample oxidizer. Recovery of radioactivity from the sample oxidizer was approximately 95% and higher. Oxidized samples as well as triplicate aliquots of the $^{14}\text{CO}_2$ trapping solution (1 ml) and urine (50 μl) were mixed with Ecolume or Ultima Gold and counted in directly in a Beckman Model LS 9800 scintillation counter (Beckman Instruments, Fullerton, CA).

HPLC Analysis of Plasma and Liver Homogenates: The metabolite profile of plasma and liver samples from WT and CYP2E1-null mice treated with 100 mg/kg for 24 hr were analyzed by HPLC. Individual plasma samples were centrifuged at 14,000xg for 20 min at 4°C and 100 µl of supernatant were directly injected into the HPLC. Liver specimens of approximately 200 mg were homogenized in sodium phosphate buffer (pH 7) at a 2:3 ratio, centrifuged at 14,000xg for 20 min at 4°C and 100 µl of the supernatant were injected into the HPLC. The HPLC system consisted of a Waters 2690 Separations Module (Waters Corporation, Milford, MA) connected on line with a UV detector followed by a 515T Radiomatic Flow Scintillation Analyzer for detection of radioactivity (Packard Instrument Co., Meriden, CT). Samples were analyzed using a 4.6 x 250 mm C18 Microsorb-MV column (Rainin Instrument Co., Woburn, MA) preceded by a security guard column (Phenomenex, Torrance, CA) using a linear gradient consisting of 100% 0.1% trifluoroacetic acid to 70% acetonitrile:30 % trifluoroacetic acid over 25 min at a flow rate of 1 ml/min. UV absorbance was monitored at 254 nm. Radioactive peaks were detected using a 500 ul flow cell with Ultima Flo-M scintillation fluid (Packard Instrument Co., Meriden, CT) at 3 ml/min.

Pharmacokinetic Analysis of Urethane Metabolism: A pharmacokinetic model was developed to assess the contribution of each enzymatic system to the metabolism of urethane. Mathematically, individual compartments depicted the production of CO₂ via specific pathways (Figure 2). Each enzymatic reaction was modeled by a first order equation. The first order constants were set as k_1 , k_2 , and k_3 for metabolism by CYP2E1, other P450 enzymes, and esterase, respectively.

Therefore, the mass balance for the body dose was modeled as:

$$d\text{Dose}/dt = -k_1 \cdot \text{Dose} - k_2 \cdot \text{Dose} - k_3 \cdot \text{Dose} .$$

The production of CO₂ by each enzymatic system (Figure 2) was then modeled as the integral of the related rate equation describing specific reactions as follows:

$$\text{CYP2E1 metabolism alone: } \text{CO}_2_{\text{CYP2E1}} = \int k_1 \cdot \text{Dose}$$

$$\text{Other P450 enzymes: } \text{CO}_2_{\text{other P450}} = \int k_2 \cdot \text{Dose}$$

$$\text{Esterase: } \text{CO}_2_{\text{est}} = \int k_3 \cdot \text{Dose}$$

The cumulative production of CO₂ by CYP2E1, other P450 enzymes, and esterase, are represented by CO₂_{CYP2E1}, CO₂_{other P450}, and CO₂_{est}, respectively. Estimates of the first order kinetic constants (k's) were performed by fitting the model simulations to the experimental data using the ACSL software (AEGIS Simulation, Inc., Huntsville, Alabama). Determinations of the k constants yielded estimates for urethane half-life based on CO₂ exhalation data. Two half-lives were estimated; for the wild-type mice as $t_{1/2} = 0.693 / (k_1 + k_2 + k_3)$, and for the CYP2E1-null mice as $t_{1/2} = 0.693 / (k_2 + k_3)$.

Statistical Analysis: Group mean comparisons were performed using Student's *t* test.

Values were considered statistically significant at $P \leq 0.05$.

Results

Exhalation of Urethane-derived $^{14}\text{CO}_2$

WT mice treated with either 10 mg/kg or 100 mg/kg [carbonyl- ^{14}C]urethane exhaled $^{14}\text{CO}_2$ in a dose-dependent manner (Figure 3). Regardless of the dose, exhalation of urethane-derived $^{14}\text{CO}_2$ in wild-type mice plateaued at 6-8 hr and was approximately 91-93% of the administered dose (Figure 3B and Table 1). In comparison to wild-type mice, significant decreases in urethane-derived $^{14}\text{CO}_2$ exhalation were observed in both the 10 and 100 mg/kg treated CYP2E1-null mice (Figure 3). Further, exhalation of $^{14}\text{CO}_2$ in KO mice was time-dependent (Table 2). Calculation of the rate of $^{14}\text{CO}_2$ exhalation (% dose/hr) in mice showed that while the rate of $^{14}\text{CO}_2$ exhalation was less than 0.05% of dose/hr between 8 and 24 hr in WT mice, it remained greater than 1.2% of dose/hr in CYP2E-null mice (data not shown). We therefore decided to assess urethane metabolism in KO mice over a 72 hr period. Approximately 70% of the administered low and high urethane doses were eliminated as $^{14}\text{CO}_2$ over a 72 hr period (Figure 3A and Table 2). Further, the rate of $^{14}\text{CO}_2$ elimination remained relatively high and was approximately 0.25% of dose/hr in KO mice at the end of the 72 hr holding period, especially, at the high dose (Figure 3A).

These data clearly showed that slow but significant metabolism of urethane to $^{14}\text{CO}_2$ occurs in CYP2E1-null mice which suggests that other enzymes continue to metabolize urethane to $^{14}\text{CO}_2$ at a slow rate for up to 72 hr in the absence of the CYP2E1 gene. It was therefore decided to assess the role of P450s other than CYP2E1 in urethane metabolism. Treatment of wild-type mice with ABT (a universal inhibitor of P450s) prior to the administration of 10 mg urethane/kg caused a drastic inhibition of urethane

metabolism to $^{14}\text{CO}_2$ (Figure 4 and Table 1). Additionally, a significant decrease in $^{14}\text{CO}_2$ exhalation occurred in KO mice-pretreated with ABT in comparison to KO mice that received urethane alone (Table 1). PAX (an inhibitor of cholinesterase) pretreatment of wild-type mice caused an initial delay in $^{14}\text{CO}_2$ exhalation during the first 6 hr after dosing as evident from comparing the slope of the elimination vs. time curves (Figure 4). Overall, however, total $^{14}\text{CO}_2$ exhalation in these animals was statistically similar to that determined at the end of the 24 hr holding period in wild-type mice treated with urethane alone (Table 1). Similarly, CYP2E1-null mice pretreated with PAX exhibited an early inhibition in $^{14}\text{CO}_2$ exhalation. However, recovery was observed by 24 hr with the total % of dose exhaled as $^{14}\text{CO}_2$ comparatively similar to that determined in CYP2E1-null mice treated with urethane alone (Figure 4 and Table 1).

Estimations of the first order pharmacokinetic constants (k's) and half-life for each metabolic pathway

The pharmacokinetic model was simulated against $^{14}\text{CO}_2$ exhalation data from wild-type, CYP2E1-null, and ABT-pretreated mice. Whenever applicable, simulations for both administered doses, 10 and 100 mg carbonyl-labeled urethane/kg b.wt. were conducted against available experimental data (Figure 5). Initial model fitting was performed on the data set for the ABT-pretreated mice. This data set depicted the production of $^{14}\text{CO}_2$ from urethane by esterase only, allowing for the estimation of k_3 . Using the determined k_3 value, the data set for the CYP2E1-null mice was then used to calculate k_2 . In CYP2E1-null mice, esterase and P450s other than CYP2E1 were responsible for the production of $^{14}\text{CO}_2$ from urethane. Lastly, determination of k_1 was

performed using data collected from the wild-type mice (CYP2E1, other P450s and esterase were functional) and the previously determined k_2 and k_3 . Model simulations against each data set are shown in Figure 5A-C. The inhibitory effects of ABT have diminished by 24 hrs according to Figure 5C. With the exception of this time point, the model simulation exhibited an excellent fit with the data. The failure of the model simulation (in ABT-pretreated mice) to fit the 24 hr time point may be attributed to the short half-life of ABT (8 hr) (Meschter *et al.*, 1994); which may indicate that the inhibitory effect of ABT declined at the 24 hr time point. Using the ACSL software, k_1 (CYP2E1), k_2 (other P450s), and k_3 (esterase) were estimated to be 0.85 hr^{-1} , 0.028 hr^{-1} , and 0.0035 hr^{-1} , respectively. Half-lives of urethane were based on $^{14}\text{CO}_2$ exhalation data and were estimated to be 0.8 hr for wild-type and 22 hr for CYP2E1-null mice.

Urethane-derived Radioactivity Exhaled as Organic Volatiles

While less than 1% of the dose was eliminated as organic volatiles in the expired air in wild-type mice, CYP2E1-null mice eliminated a significantly greater portion of the dose (3-4%) via the same route (Table 1). In comparison, at 72 hours after urethane administration of 10 or 100 mg/kg, 8 and 5% of the low and high doses were exhaled as organic volatiles, respectively. These values were significantly higher than those determined at 24 hours (Table 2). Additionally, pretreatment of mice with ABT or PAX resulted in a small increase in the % of dose exhaled as organic volatiles (Table 1). Preliminary HPLC analysis of charcoal trap extracts suggested that urethane was present in the expired air of CYP2E1-null mice. Additional work is currently in progress to identify other exhaled organic volatiles.

Urinary and Fecal Excretion of Urethane-derived Radioactivity

While there were no significant differences in the excretion of urethane-derived radioactivity in the urine of mice of either genotype treated with 100 mg/kg urethane for 24 hr, a significant increase was observed in KO mice administered 10mg/kg vs. wild-type mice (2 vs. 6% of dose, Table 1). Urinary excretion of urethane-derived radioactivity at 72 hr (9-10% of dose) after dosing was statistically similar regardless of dose (Table 2). However, when compared with that at 24 hr, the % of urethane dose excreted in the urine at 72 hr. was doubled (Table 2). The effect of ABT and PAX on the excretion of urethane-derived radioactivity in the urine of mice of both genotypes was shown in Table 1. Although ABT increased the urinary excretion of urethane-derived radioactivity in wild-type mice, it resulted in a negligible change in urethane urinary elimination in KO mice (Table 1). Inhibition of esterase in CYP2E1-null or wild-type mice by PAX showed a significant decrease in the amount of urethane-derived radioactivity excreted in the urine (Table 1). Using HPLC analyses, approximately 70% of the total amount of urethane-derived radioactivity excreted in the urine of CYP2E1-null mice was identified as parent urethane. However, HPLC analyses of urine collected from wild-type mice demonstrated that parent compound accounted for approximately 15% of total urethane-derived radioactivity. Furthermore, the decrease in urethane in the urine of wild-type mice was associated with an increase in an early eluting metabolite with an opposite pattern in CYP2E1-null mice (approximately 65% of dose in wild-type vs. 13 % of dose in CYP2E1-null mice). Overall, fecal excretion of urethane-derived radioactivity was negligible in all groups (Table 1 and 2).

Analysis and Identification of Urethane-derived Radioactivity in Blood and Tissues

In general, tissue and blood concentrations of urethane-derived radioactivity increased in a dose-dependent manner, achieving a maximum within 24 hr, and declining at 72 hr after dosing in each of the 2 mice genotypes (Tables 3). Moreover, tissue and blood concentrations of urethane-derived radioactivity were significantly higher in CYP2E1-null vs. wild-type mice in all treatment groups (Table 4). However, the effect of ABT was more pronounced than that of PAX (Table 4). Fractionation of blood and subsequent analysis demonstrated that the concentration of urethane derived radioactivity in whole blood, plasma and red blood cells (48-52 μg urethane/g blood or ml plasma) were essentially similar in the 100mg/kg CYP2E1-null mice. In contrast, wild-type mice administered the same dose contained an approximately 2-fold increase in urethane-derived radioactivity in red blood cells vs. plasma (1.75 vs. 0.83 μg urethane/g or ml). HPLC analysis of the plasma of CYP2E1-null mice at 24 hr after the administration at 100 mg/kg surprisingly showed that urethane was the only radiolabeled chemical detectable in the plasma. Subsequently, analysis of liver homogenates from these mice also showed that urethane was the only detectable radiolabeled chemical.

Discussion

Urethane is a documented multi-site carcinogen capable of inducing a host of tumor types in various organs and animal species. Potential human exposure via the consumption of foods containing urethane and its ability to cause tumorigenesis in animals has prompted extensive investigations into urethane's mechanism(s) of action. Currently, the accepted hypothesis centers on the assumption that while urethane metabolism via esterase is the primary pathway, activation of this chemical via CYP2E1 to vinyl carbamate, and subsequently to vinyl carbamate epoxide, is a pre-requisite for tumor development. Most studies addressing this hypothesis, however, relied on the use of enzyme modulators. Generally, inhibitors/inducers of metabolism produce inconclusive results, affecting not only their intended targets, but also altering other enzymes and normal biochemical/physiological processes (Ghanayem *et al.*, 2000). With the advent of genetically engineered mice, the effect of a single enzyme on the bioactivation and/or detoxification of a xenobiotic can be directly determined (Gonzalez 1998; Gonzalez and Kimura 1999; Ghanayem *et al.*, 2000). Therefore, the overall objective of ongoing research in this laboratory is to assess the relationships between urethane metabolism, and toxicity, mutagenicity, and carcinogenicity. Present work focuses on the assessment of the role of CYP2E1 in urethane metabolism using CYP2E1-null and wild-type mice.

Current results showed that urethane was rapidly absorbed and distributed to all major tissues of mice. However, significant differences in urethane metabolism were observed in wild-type and CYP2E1-null mice. Regardless of dose, 91-93% of administered urethane was metabolized to $^{14}\text{CO}_2$ and eliminated in expired air in wild-

type mice within 6 hr. In contrast, a greater than 6-fold decrease in exhaled $^{14}\text{CO}_2$ was observed in CYP2E1-null mice treated with urethane indicating that CYP2E1 was the principal enzyme responsible for urethane metabolism. These findings are in stark contrast to previous studies reporting esterase as the primary enzyme responsible for urethane metabolism to $^{14}\text{CO}_2$. Although limited intercrossing of 129/Sv and C57BL/6N in the current studies may have produced wild-type and CYP2E1-null mice with different genetic backgrounds, in turn affecting the present results, strong evidence suggested otherwise. Clear differences in urethane metabolism between wild-type and CYP2E1-null mice regardless of dose, small animal to animal variations within treated groups, and the strong agreement of the current results with earlier studies that used various mouse strains argues against non-uniform genetic backgrounds influencing urethane metabolism in the present study. Skipper et al (1951) showed that within 24 hr after a single radiolabeled urethane dose had been administered intraperitoneally to CFW mice, greater than 95% of the dose was eliminated as expired $^{14}\text{CO}_2$. Nomier et al (1989) demonstrated that greater than 90% of administered oral or iv doses of [carbonyl- ^{14}C]-urethane was exhaled by B6CF31 mice as $^{14}\text{CO}_2$ within 4 hr. Furthermore, elimination of $^{14}\text{CO}_2$ in the expired air of male A/ Jax mice constituted approximately 85% of an oral dose of urethane (Yamamoto et al 1988, 1990). An IARC review of available studies concluded that regardless of the route of exposure, urethane undergoes rapid systemic distribution and approximately 90% of a given dose would be excreted as exhaled $^{14}\text{CO}_2$ within 24 hr (IARC 1974). More recently, subsequent studies performed in this laboratory comparing the metabolism and disposition of carbonyl and ethyl-labeled urethane in CYP2E1-null and wild-type mice

yielded relatively identical results to present data (Hoffler and Ghanayem 2002). Clearly, present and earlier studies are in agreement that biotransformation of urethane to $^{14}\text{CO}_2$ in mice was not significantly affected by mouse strain.

Current results unquestionably showed CYP2E1 was the principal enzyme responsible for the metabolism of [carbonyl- ^{14}C]-urethane. Furthermore, these data demonstrated that CYP2E1's absence caused a dramatic increase in urethane's half-life (0.8 hr in wild-type and 22 hr in CYP2E1-null mice) and may lead to urethane bioaccumulation upon multiple dosing. Present work also suggested that additional enzymes, other than CYP2E1, were participating in urethane metabolism. Using the universal P450 inhibitor, ABT, the role of all P450s was examined. Pretreatment of mice with ABT resulted in significant reduction in urethane metabolism to CO_2 and rendered both genotypes of mice metabolically similar. However, these results suggested that the involvement of other P450s was minimal compared to the contribution of CYP2E1. Because urethane's metabolism to CO_2 was not entirely inhibited by ABT, it was hypothesized that non-P450s such as esterase were involved. Urethane is an aliphatic ester and is susceptible to esteric cleavage by esterases. Previous work by Yamamoto *et al* (1990) showed that pretreatment of A/Jax mice with PAX, a cholinesterase inhibitor, caused a significant increase of urethane-derived radioactivity in the blood 2 hr after urethane administration. In the present study, the rate of urethane metabolism to CO_2 was initially inhibited in PAX-pretreated mice. Recovery, however, was observed within 24 hr, suggesting that PAX-mediated inhibition of esterase was transient. Ironically, urinary excretion of urethane-derived radioactivity was significantly reduced in both PAX-pretreated CYP2E1-null and wild-

type mice. Whether this decrease means that the majority of urinary metabolites derived from urethane originate from pathways mediated by esterase remains to be determined. Preliminary HPLC analysis of urine showed significant presence of parent urethane in the urine of CYP2E1-null vs. wild-type mice.

To assess the contributions of CYP2E1, other P450s, and esterase in the metabolism of urethane, a pharmacokinetic model was simulated against actual CO₂ exhalation data from wild-type, CYP2E1-null, and ABT-pretreated mice. First order kinetic constants (k's) were calculated for each metabolic pathway. Generally, the model simulation exhibited an excellent fit with the experimental data. Initial modeling was performed on the data from ABT-pretreated mice. This data set depicted the production of CO₂ from urethane via esterase and revealed that esterase contribution was negligible, accounting for less than 0.5% of an administered dose ($k=0.0035 \text{ hr}^{-1}$). The failure of the model prediction to fit the 24 hr time point may be attributed to ABT's short half-life (8 hr) in mice (Meschter *et al.*, 1994). Therefore, the inhibitory effect of ABT may decline, resulting in an underestimation by the model. In CYP2E1-null mice, esterase and P450s (other than CYP2E1) were responsible for the production of CO₂. The rate constant for these P450s was calculated and revealed that the contribution of these enzymes to urethane metabolism to CO₂ was approximately 3.2% of an administered dose ($k=0.028 \text{ hr}^{-1}$). In wild-type mice, CYP2E1, other P450s, and esterase were responsible for urethane metabolism to CO₂. Using the rate constants for esterase and other P450s, the rate constant for CYP2E1 was calculated ($k=0.85 \text{ hr}^{-1}$). Greater than 96% of urethane metabolism to CO₂ was attributed to CYP2E1.

Blood and tissue concentrations of urethane-derived radioactivity were dose-dependent in mice. Interestingly, tissue and blood levels of urethane remained elevated even at 72 hr after chemical administration to CYP2E1-null mice. Therefore, in the absence of CYP2E1-mediated metabolism, urethane clearance was drastically inhibited and its half-life dramatically increased. Furthermore, retention of radioactivity in tissues and blood was potentiated in both CYP2E1-null and wild-type mice after pretreatment with either ABT or PAX. Notably, these results contradict the assumption that radioactivity in tissues was the result of re-incorporation of $^{14}\text{CO}_2$ and ethanol (Skipper *et al.*, 1951; Salmon and Zeise 1991). Moreover, these data may contradict the suggestion that elevated levels of urethane-derived radioactivity in tissues resulted from covalent binding of metabolites originating via CYP2E1-mediated oxidation (Salmon and Zeise 1991). Especially, since inhibition of urethane oxidation in CYP2E1-null and in ABT-pretreated mice was associated with higher tissue levels of urethane-derived radioactivity. In fact, HPLC analysis confirmed that urethane was the only chemical detectable in the blood and liver of CYP2E1-null mice treated with this chemical.

In conclusion, urethane was rapidly absorbed and distributed to all major tissues after gavage administration. The use of CYP2E1-null mice directly demonstrated for the first time that CYP2E1 and not esterase was the principal enzyme responsible for the metabolism of [carbonyl- ^{14}C]-urethane to $^{14}\text{CO}_2$. Pharmacokinetic modeling of $^{14}\text{CO}_2$ exhalation data revealed that CYP2E1, other P450s, and esterase contribute 96.4, 3.2, and 0.4% to urethane metabolism to CO_2 , respectively, in genetically intact mice. Although model estimates suggested that contributions of P450s (other than CYP2E1) and esterase were minimal, the roles of these enzymes were exaggerated in CYP2E1-

null mice, possibly due to the increased urethane blood concentration in these animals. Absence of CYP2E1 led to a significant increase in the half-life of urethane in CYP2E1-null mice (22 hr vs. 0.8 hr in wild-type mice) and suggested that urethane bioaccumulation may occur upon multiple exposures. Polymorphisms in CYP2E1 may enhance or reduce a person's predisposition to cancer. As reported by Marchand *et al* (1998), CYP2E1 *RsaI* and *DraI* polymorphisms were associated with a 10-fold decrease in the risk of overall lung cancer (*RsaI* variant) and adenocarcinoma (*DraI* variant) compared to homozygous wild-type genotypes. Therefore urethane half-life may increase in humans with polymorphisms that decrease basal CYP2E1 metabolic activity. However, it remains to be determined if a decrease in urethane metabolism in exposed humans results in the induction of toxic/ carcinogenic effects by unmetabolized urethane or by metabolites formed via other pathways. Additional work is currently in progress to determine whether inhibition of urethane metabolism in CYP2E1-null mice may influence the mutagenicity and carcinogenicity of this chemical.

Acknowledgements

We would like to thank Drs Tom Burka, Michael Kohn, Trinia Simmons, Ghanta Rao, Yuji Mishini and J. Michael Sanders for their comments, suggestions, and discussion.

In addition, we would like to thank Dr. Frank Gonzalez for providing us with the animals to establish our breeding colony of CYP2E1-null and wild-type mice, as well as Brian Chanas for his technical assistance.

References

Benson RW and Beland FA (1997) Modulation of urethane (ethyl carbamate) carcinogenicity by ethyl alcohol: A review. *International Journal of Toxicology* **16**(6): 521-544.

Dahl G, Miller JA, and Miller EC (1978) Vinyl Carbamate as a promutagen and a more carcinogenic analog of ethyl carbamate. *Cancer Research* **38**: 3793-3804.

Forkert PG and Lee RP (1997) Metabolism of ethyl carbamate by pulmonary cytochrome P450 and carboxylesterase isozymes: involvement of CYP2E1 and hydrolase A. *Toxicol Appl Pharmacol* **146**(2): 245-254.

Ghanayem BI, Wang H, and Sumner S (2000) Using cytochrome P-450 gene knock-out mice to study chemical metabolism, toxicity, and carcinogenicity. *Toxicol Pathol* **28**(6): 839-850.

Gonzalez FJ (1998) The study of xenobiotic-metabolizing enzymes and their role in toxicity in vivo using targeted gene disruption. *Toxicol Lett* **102-103**: 161-166.

Gonzalez FJ and Kimura S (1999) Role of gene knockout mice in understanding the mechanisms of chemical toxicity and carcinogenesis. *Cancer Lett* **143**: 199-204.

Guengerich FP and Kim DH (1991) Enzymatic oxidation of ethyl carbamate to vinyl carbamate and its role as an intermediate in the formation of 1, N⁶- Ethenoadenosine. *Chem Res Toxicol* **4**(4): 413-421.

Hoffler U and Ghanayem BI (2002) Comparison of the disposition of ethyl and carbonyl-labeled urethane in CYP2E1-null (KO) vs. wild-type (WT) mice. *Presented at the XIVth World Congress of Pharmacology: IUPHAR abstract.*

IARC (1974) *Urethane. In monographs on the carcinogenic risk of chemicals to man: some antithyroid and related substances, nitrofurans and industrial chemicals.* Lyon, France, International Agency for Research on Cancer. **7**: 111-140.

Kaye AM (1960) A study of the relationship between the rate of ethyl carbamate (urethane) catabolism and urethane carcinogenesis. *Cancer Res* **20**: 237-241.

Lee RP, Parkinson A, and Forkert PG (1998) Isozyme-selective metabolism of ethyl carbamate by cytochrome P450 (CYP2E1) and carboxylesterase (hydrolase A) enzymes in murine liver microsomes. *Drug Metab Dispos* **26**(1): 60-65.

Lee SST, Buters JTM, Pineau T, Fernandez-Salguero P, and Gonzalez FJ. (1996) Role of CYP2E1 in the hepatotoxicity of acetaminophen. *J. Biol. Chem.* 271:12063-12067.

Marchand L, Sivaraman L, Pierce L, Seifried A, Lum A, Wilkens LR, and Lau AF (1998) Associations of CYP1A1, GSTM1, and CYP2E1 polymorphisms with lung cancer suggest cell type specificities to tobacco carcinogens. *Cancer Res* **58**: 4858-4863.

Meschter CL, Mico BA, Mortillo M, Garland WA, Riley JA, and Kaufman LS (1994) A 13-week toxicologic and pathologic evaluation of prolonged cytochromes P450 inhibition by 1- aminobenzotriazole in male rats. *Fund. Appl. Tox.* **22**: 369-381.

Mirvish SS (1968) The carcinogenic action and metabolism of urethane and N-hydroxyurethane. *Adv. Cancer Res.* **11**:1-42.

Nettleship AH, Henshaw PS, and Meyer HL (1943) Induction of Pulmonary Tumors in Mice with Ethyl Carbamate. *J. Natl. Cancer Inst.* **4**: 309-319.

Nomeir AA, Ioannou YM, Sanders JM, and Matthews HB (1989) Comparative metabolism and disposition of ethyl carbamate (urethane) in male Fischer 344 rats and male B6C3F1 mice. *Toxicol Appl Pharmacol* **97**(2): 203-215.

Nomura T (1975) Transmission of tumors and malformations to the next generation of mice subsequent to urethane treatment. *Cancer Res* **35**: 264-266.

National Toxicology Program (NTP) (2000) *Report on Carcinogens*, 9th Edition. RTP, NC, National Institute of Environmental Health Sciences, National Institutes of Health.

Page DA and Carlson GP (1994) The effect of pyridine on the *in vitro* and *in vivo* metabolism of ethyl carbamate (urethane) by rat and mouse. *Carcinogenesis* **15**(10): 2177-2181.

Ribovich ML, Miller JA, Miller EC, and Timmins LG (1982) Labeled 1,N⁶-ethenoadenosine and 3,N⁴-ethenocytidine in hepatic RNA of mice given [Ethyl-1,2-³H or Ethyl-1-¹⁴C] Ethyl Carbamate (Urethane). *Carcinogenesis* **3**(5): 539-546.

Salmon A and Zeise L (1991) *Risks of Carcinogenesis from Urethane Exposure*. Boca Raton, Fl, CRC Press, Inc.

Schlatter J and Lutz WK (1990) The carcinogenic potential of ethyl carbamate (Urethane) - risk assessment at human dietary exposure levels. *Food and Chemical Toxicology* **28**(3): 205-211.

Schmahl D, Port R, and Wahrendorf J (1977) A dose-response study on urethane carcinogenesis in rats and mice. *Int. J. Cancer* **19**: 77-80.

Skipper HE, Bennett LL Jr, Bryan CE, White L Jr, Newton MA, Simpson L (1951). Carbamates in the chemotherapy of leukemia. VIII. Over-all tracer studies on carbonyl- labeled urethane, methylene- labeled urethane and methylene- labeled ethyl alcohol. *Cancer Res* **11**: 46-51.

U.S. Department of Health and Human Services, National Institutes of Health (1985) *Guide of the Care and Use of Laboratory Animals*. NIH Publication no.86-23, National Institutes of Health, Bethesda, MD.

Wang H, Chanas B, Ghanayem BI (2002) Cytochrome P450 2E1 (CYP2E1) is essential for acrylonitrile metabolism to cyanide: comparative studies using CYP2E1-null and wild-type mice. *Drug Metab Dispos* **30**(8): 911-917.

Yamamoto T, Pierce WM Jr, Hurst HE, Chen D, and Waddell WJ (1988) Inhibition of the metabolism of urethane by ethanol. *Drug Metab Dispos* **16**(3): 355-358.

Yamamoto T, Pierce WM Jr, Hurst HE, Chen D, and Waddell WJ (1990) Ethyl carbamate metabolism – *in vivo* Inhibitors and *in vitro* enzymatic systems. *Drug Metab Dispos* **18**(3): 276-280.

Zimmerli B, Baumann U, Nägeli P, and Battaglia R (1986) Occurrence and formation of ethylcarbamate (urethane) in fermented foods. Some Preliminary results. *Proceedings of Euro Food Tox II* 243-248.

Footnotes

The presented work is in partial fulfillment of Undi Hoffler's Ph.D. dissertation research.

Portions of this work were presented at the 41st Annual Society of Toxicology meeting in Nashville, TN, March 2002

Figure Legends

Figure 1. A proposed scheme of Urethane metabolism

Figure 2. A proposed compartmentalized model describing urethane metabolism to CO₂ via specific enzymatic pathways (including associated first order kinetic constants).

Figure 3. A. Effects of dose and genotype on the exhalation of ¹⁴CO₂ in CYP2E1^{-/-} and CYP2E1^{+/+} mice after gavage administration of ¹⁴C-carbonyl labeled urethane as a function of time. All values are presented as cumulative % of dose. CYP2E1^{-/-} values for time points during the 1st 24 hr are the mean ± SE of 8 mice. CYP2E1^{+/+} values are the mean ± SE of 3-4 mice. ^a denotes statistical significance of ¹⁴CO₂ elimination by mice at 100mg/kg; ^b denotes statistical significance at 10mg/kg; ^c denotes a statistical difference in the 2nd hour value between the 10 and 100 mg/kg treated wild-type mice.

B. Effects of dose and genotype on the exhalation of ¹⁴CO₂ in CYP2E1^{-/-} and CYP2E1^{+/+} mice treated with ¹⁴C-carbonyl labeled urethane by gavage as a function of time. All values are presented as cumulative % of dose. CYP2E1^{-/-} values for time points during the 1st 24 hr are the mean ± SE of 8 mice. CYP2E1^{+/+} values are the mean ± SE of 3-4 mice. ^c denotes a statistical difference in the 2nd hour value between the 10 and 100 mg/kg treated wild-type mice.

Figure 4. Effects of 1-aminobenzotriazole (ABT) and paraoxon (PAX) on the exhalation of ¹⁴CO₂ in CYP2E1^{-/-} and CYP2E1^{+/+} mice after gavage administration of 10 mg/kg ¹⁴C-labeled urethane as a function of time. All values are presented as cumulative % of dose. Values from CYP2E1^{-/-} mice administered urethane only are

the mean \pm SE of 8 mice. The remaining values are the mean \pm SE of 3-4 mice. ^adenotes statistical significance of ¹⁴CO₂ elimination by the 2 genotypes of mice at 10mg/kg; ^bdenotes statistical comparison of values from KO mice with and without PAX; ^cdenotes statistical comparison of values from mice of both genotypes with and without ABT.

Figure 5. Pharmacokinetic model simulations of the experimental CO₂ exhalation data from 100 mg/kg wild-type (●) and CYP2E1-null mice (*), (Panel A); 10 mg/kg wild-type (□) and CYP2E1-null mice (▲), (Panel B); and ABT-pretreated wild-type (■) and CYP2E1-null mice (†), (Panel C). The lines represent the results of the model simulations and the symbols represent the actual experimental CO₂ production data from mice treated with urethane (U). N=8 for the CYP2E1-null mice and 3-4 for all other groups.

Table 1:

Summary of [Carbonyl- ¹⁴ C]Urethane(U) Disposition within 24 hours after gavage administration								
	100mgU/kg		10mg U/kg		ABT+10mg U/kg		PAX+10mg U/kg	
	WT (n=4)	KO (n=8)	WT (n=4)	KO (n=8)	WT (n=3)	KO (n=4)	WT (n=4)	KO (n=4)
CO ₂	95.0±5.2	44.4±4.3 ^a	91.9±2.7	39.7±3.0 ^a	13.0±2.3 ^b	14.6±0.9 ^b	96.0±1.2	35.1±1.7 ^a
Organic Volatiles	0.5±0.2	2.6±0.9 ^a	0.2±0.1	3.8±1.0 ^a	3.6±0.1 ^b	3.2±1.6	0.7±0.1 ^b	4.9±0.1
Urine	3.5±1.2	5.0±1.6	2.3±0.4	5.9±1.7 ^a	4.8±0.6 ^b	4.2±0.3	0.2±1.0 ^b	1.1±1.2 ^b
Feces	<i>neg</i>	<i>neg</i>	<i>neg</i>	<i>neg</i>	<i>neg</i>	<i>neg</i>	<i>neg</i>	<i>neg</i>
Total % of dose	99.0	52.0	94.4	49.4	21.4	22.0	96.9	41.1
Values are presented as cumulative % of dose and are the mean±SE. ^a denotes KO values that are statistically significant from corresponding WT values (P≤0.05). ^b denotes pretreatment values that are statistically significant from corresponding U treatment only (P≤0.05). Negligible (<i>neg</i>) values were less than 1%. Abbreviations: U, Urethane; KO, CYP2E1-null mice; WT, wild-type mice; ABT, 1-aminobenzotriazole; PAX, paraoxon.								

Table 2:

<i>Effect of Time on the Disposition of [Carbonyl-¹⁴C]Urethane (U) in Male CYP2E1-Null Mice within 24 and 72 hours after Gavage administration</i>				
	24 hours (n=8)		72 hours (n=4)	
	10mg U/kg	100mg U/kg	10mg U/kg	100mg U/kg
CO ₂	39.7 ± 2.9	44.4 ± 4.3	68.9 ± 1.0 ^a	68.2 ± 1.6 ^a
Organic Volatiles	3.8 ± 1.0	2.6 ± 0.9	7.7 ± 1.1 ^a	5.0 ± 0.6 ^a
Urine	5.9 ± 1.7	5.0 ± 1.6	9.8 ± 1.3 ^a	9.3 ± 0.9 ^a
Feces	<i>neg</i>	<i>neg</i>	<i>neg</i>	<i>neg</i>
Total % of dose	49.4	52.0	86.4	82.5

Values are presented as cumulative % of dose and are the mean±SE. ^a denote statistically different values (P≤0.05) from corresponding 24 hour values. Negligible (neg) values were less than 1% of dose.
 Abbreviations: U, Urethane.

Table 3. Concentration of Urethane (U)-Derived Radioactivity in Tissues 24 and 72 Hours Post Gavage Administration

<i>Tissues</i>	<i>24 hour</i>				<i>72 hour</i>	
	<i>WT</i>		<i>KO</i>		<i>KO</i>	
	<i>10mg/kg</i>	<i>100mg/kg</i>	<i>10mg/kg</i>	<i>100mg/kg</i>	<i>10mg/kg</i>	<i>100mg/kg</i>
<i>Blood</i>	0.12±0.0	1.28±0.2	2.17±0.4	47.65±4.8	1.14± 0.1	8.77±0.9
<i>Brain</i>	0.04±0.0	0.71±0.3	4.35±0.2	49.97±6.7	0.61±0.0	5.84±0.3
<i>Fat</i>	0.03±0.0	0.59±0.3	0.73±0.1	9.20±2.3	0.17±0.0	4.90±1.4
<i>Forestomach</i>	0.32±0.1	4.69±1.5	3.24±1.2	41.95±9.9	0.39±0.2	2.03±0.4
<i>Glandular stomach</i>	0.13±0.0	1.81±0.3	3.50±0.6	41.30±8.2	0.20±0.0	2.68±0.7
<i>Lg. intestine</i>	0.15±0.1	2.20±0.4	4.09±0.4	48.33±4.6	0.32±0.0	3.28±0.8
<i>Sm. intestine</i>	0.15±0.0	2.82±1.1	4.50±0.3	51.31±5.1	0.38±0.1	3.55±0.3
<i>Kidneys</i>	0.13±0.0	2.19±0.5	4.68±0.3	52.77±7.0	0.69±0.0	5.65±0.6
<i>Liver</i>	0.22±0.0	2.57±0.8	4.56±0.2	48.13±0.8	0.51±0.0	4.79±0.2
<i>Lung</i>	0.08±0.0	1.46±0.2	4.71±0.3	46.45±5.1	0.46±0.2	4.50±0.1
<i>Muscle</i>	0.04±0.0	1.16±0.4	4.30±0.4	48.44±5.3	0.42±0.2	5.53±0.6
<i>Skin</i>	0.10±0.0	1.15±0.1	2.70±0.3	26.34±3.3	0.51±0.1	5.46±0.4
<i>Spleen</i>	0.08±0.0	1.61±0.3	4.69±0.2	52.30±6.2	0.63±0.0	5.50±0.5
<i>Testes</i>	0.05±0.0	1.20±0.4	4.67±0.2	49.44±2.2	0.68±0.0	6.11±0.1
<i>Thymus</i>	0.08±0.0	1.42±0.5	3.98±0.9	38.46±4.8	0.45±0.0	2.75±1.8
<i>Urinary bladder</i>	0.22±0.1	2.25±2.0	5.21±0.4	65.92±3.9	0.49±0.1	5.51±0.0

Each value represents the mean ±SE of at least 3 mice except blood at 24 hour from 100mg/kg WT and KO mice where n=7 and n=9 respectively.

All values are expressed as µg U equivalents/g tissue.

All tissue concentrations in the KO mice are statistically significant vs. WT values.

All tissue concentrations in 72 hr KO are statistically significant vs. 24 hr KO values.

Abbreviations: U, Urethane; KO, CYP2E1-null mice; WT, wild-type mice.

Table 4. Concentration of Urethane (U)-derived Radioactivity in Tissues of mice Pretreated with ABT or PAX 24 Hours After Gavage Administration of Urethane

<i>Tissues</i>	<i>WT</i>			<i>KO</i>		
	<i>10mg/kg U</i>	<i>ABT+ 10mg/kg U</i>	<i>PAX+ 10mg/kg U</i>	<i>10mg/kg U</i>	<i>ABT+ 10mg/kg U</i>	<i>PAX+ 10mg/kg U</i>
<i>Blood</i>	0.12±0.0	7.26±0.3	0.27±0.0	2.17± 0.4	8.33±1.2	6.99±0.7
<i>Brain</i>	0.04±0.0	7.65±0.3	0.19±0.1	4.35±0.2	8.30±0.9	6.70±0.1
<i>Fat</i>	0.03±0.0	1.44±0.3	0.12±0.1	0.73±0.1	1.39±0.2	1.30±0.1
<i>Forestomach</i>	0.32±0.1	0.67±0.5	1.45±0.4	3.24±1.2	7.58±2.9	5.02±0.5
<i>Glandular stomach</i>	0.13±0.0	7.78±0.3	1.11±0.2	3.50±0.6	7.41±2.3	5.13±1.6
<i>Lg. intestine</i>	0.15±0.1	7.31±0.4	0.71±0.1	4.09±0.4	8.76±0.6	7.01±0.7
<i>Sm. intestine</i>	0.15±0.0	8.79±0.1	0.72±0.1	4.50±0.3	8.45±0.2	7.06±0.6
<i>Kidneys</i>	0.13±0.0	8.09±0.5	0.67±0.2	4.68±0.3	8.68±0.8	7.23±1.0
<i>Liver</i>	0.22±0.0	7.30±0.8	0.96±0.1	4.56±0.2	8.12±0.6	6.49±0.2
<i>Lung</i>	0.08±0.0	7.97±0.2	0.40±0.2	4.71±0.3	8.97±0.3	6.78±0.0
<i>Muscle</i>	0.04±0.0	7.72±0.4	0.35±0.2	4.30±0.4	8.01±0.3	6.59±0.5
<i>Skin</i>	0.10±0.0	4.61±0.5	0.27±0.0	2.70±0.3	5.23±0.7	4.71±0.5
<i>Spleen</i>	0.08±0.0	8.34±0.3	0.34±0.1	4.69±0.2	8.74±0.5	6.74±0.2
<i>Testes</i>	0.05±0.0	8.77±0.4	0.36±0.1	4.67±0.2	8.31±0.2	6.90±0.1
<i>Thymus</i>	0.08±0.0	5.42±0.5	0.31±0.1	3.98±0.4	6.75±0.3	5.68±0.9
<i>Urinary bladder</i>	0.2±0.1	8.58±1.0	1.45±0.7	5.21±0.4	9.69±1.1	6.99±0.1

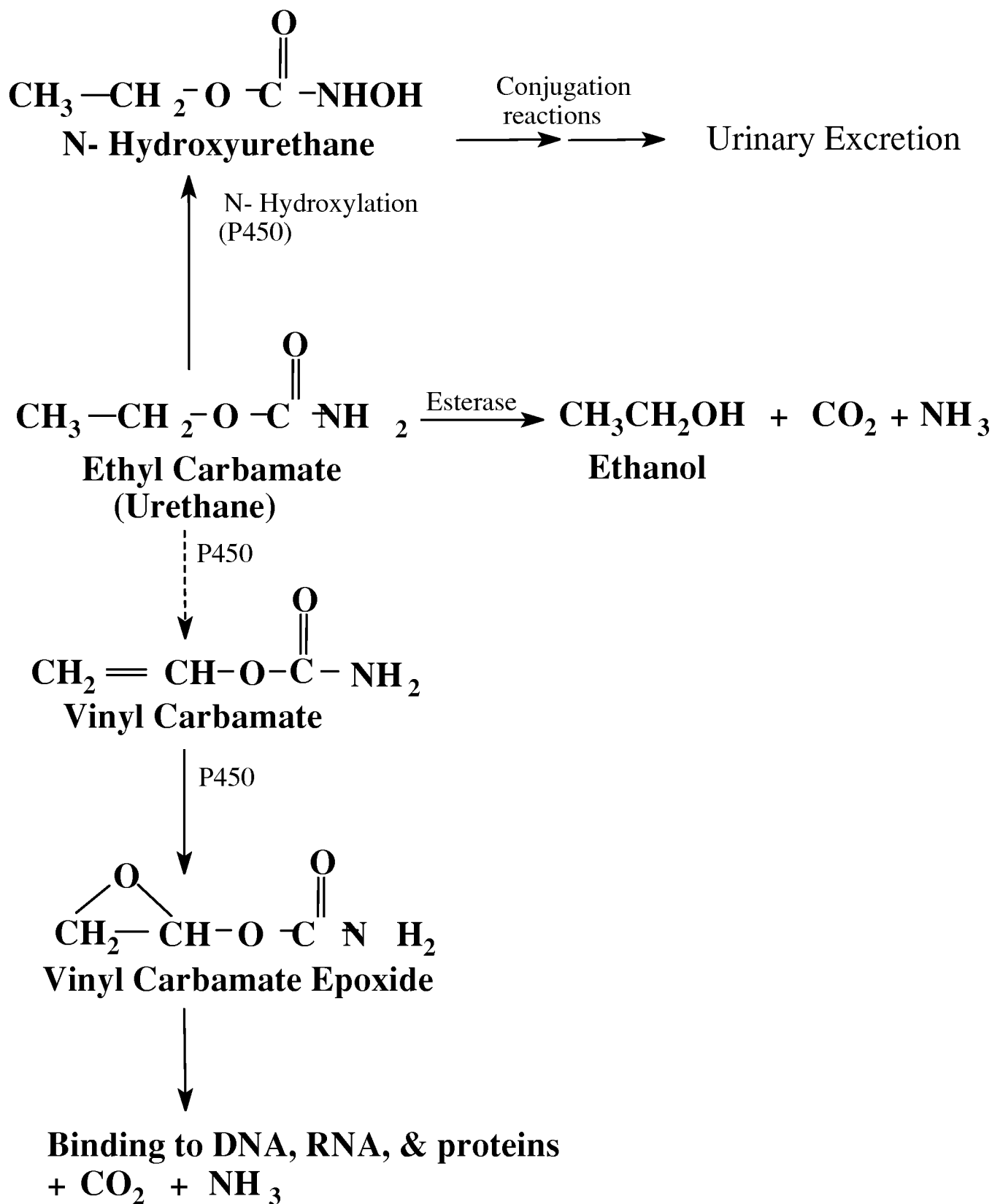
Each value represents the mean ±SE of at least 3 mice expressed as µg U equivalents/g tissue.

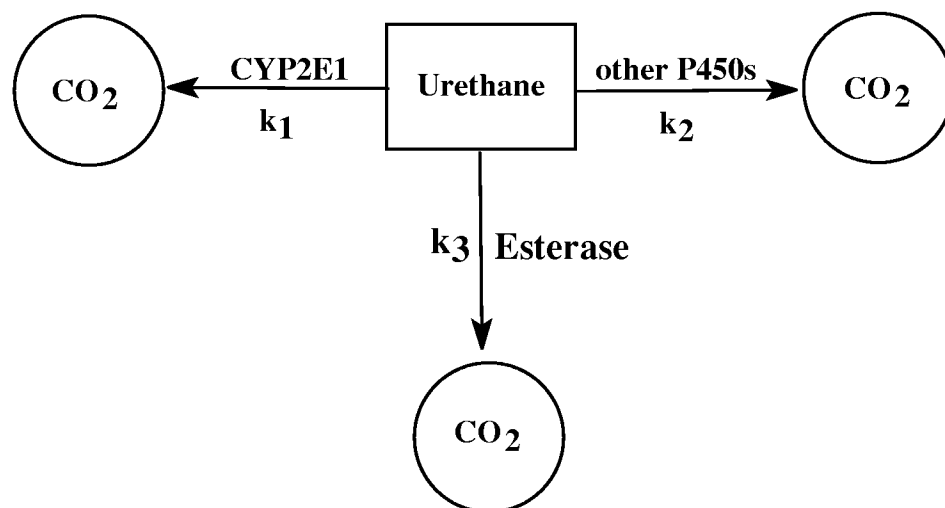
All tissue concentrations of urethane-derived radioactivity are statistically significant in ABT or PAX pretreated WT vs. U only.

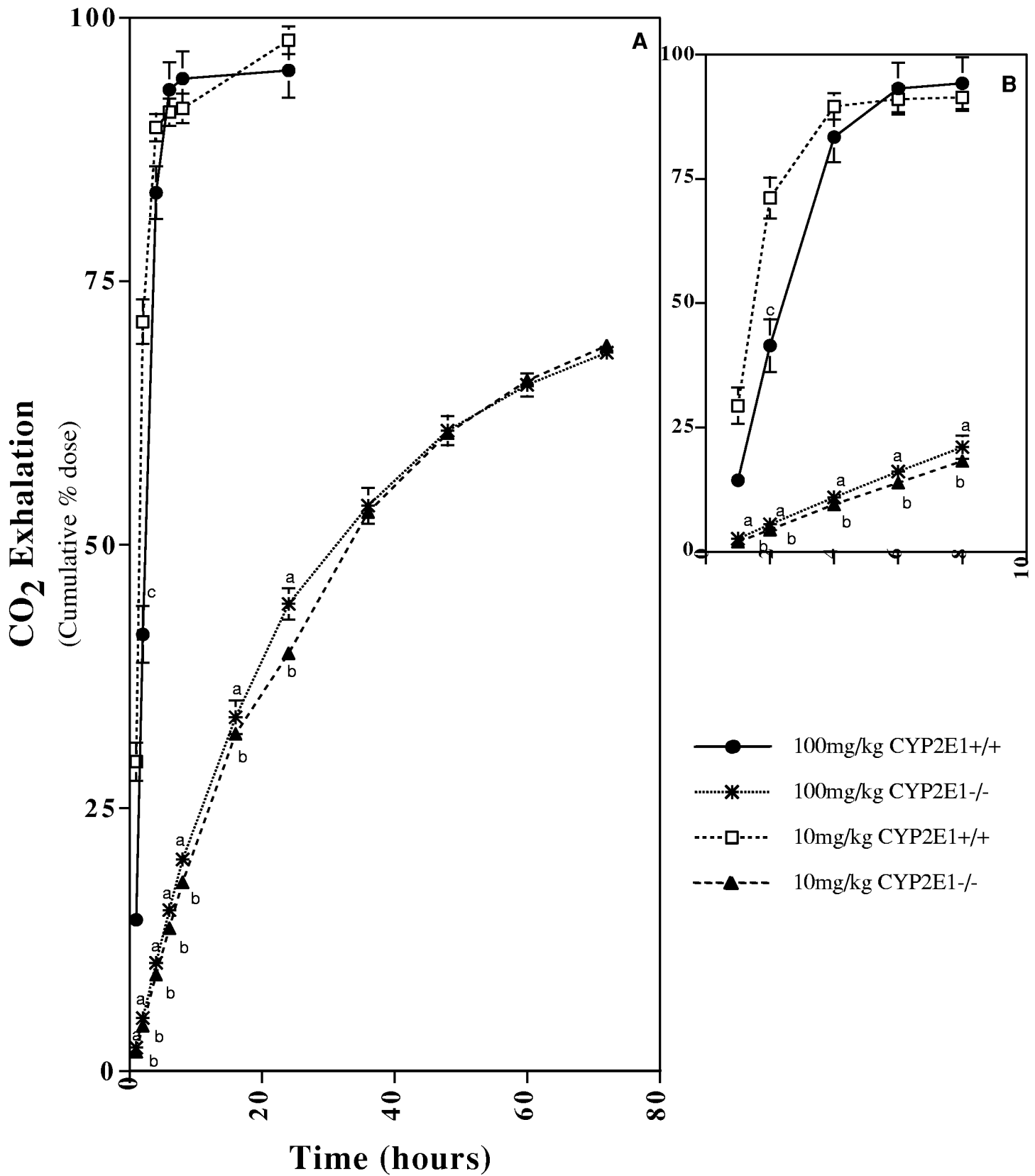
All tissue concentrations of urethane-derived radioactivity are statistically significant in ABT pretreated KO vs. U only.

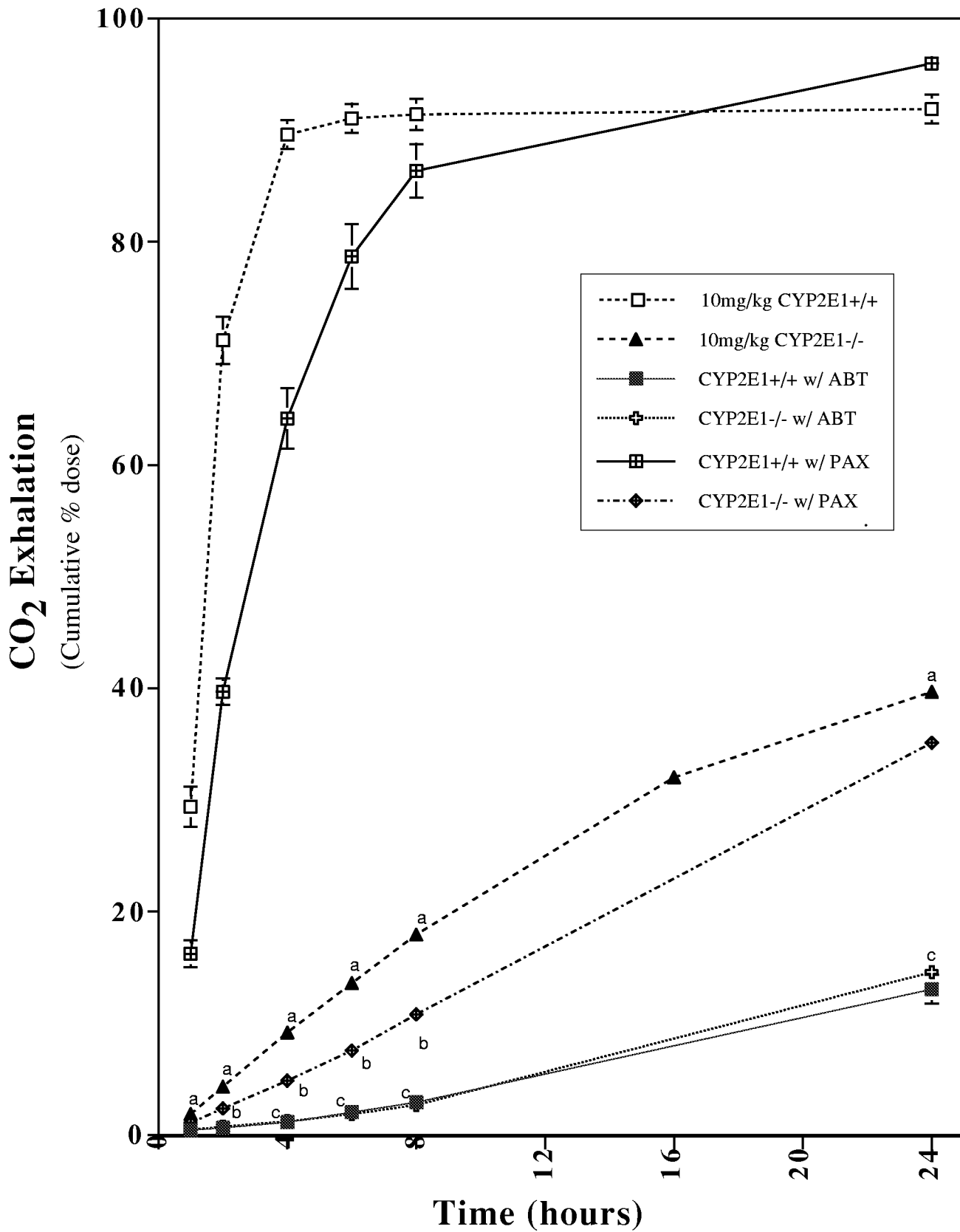
While all tissue concentrations in PAX pretreated KO are higher than U only administered KO, not all values are statistically different.

Abbreviations: U, Urethane; KO, CYP2E1-null mice; WT, wild-type mice; ABT, 1-aminobenzotriazole; PAX, paraoxon.









Cumulative CO₂ Exhalation
($\mu\text{g U equivalent}$)

